ACS OMEGA

http://pubs.acs.org/journal/acsodf

Article

Novel Drug Carrier: 5-Fluorouracil Formulation in Nanoporous Biogenic Mg-calcite from Blue Crab Shells—Proof of Concept

Geza Lazar, Fran Nekvapil, Razvan Hirian, Branko Glamuzina, Tudor Tamas, Lucian Barbu-Tudoran, and Simona Cinta Pinzaru*

Cite This: *ACS Omega* 2021, 6, 27781−27790

Read Online

ACCESS | Metrics & More | Article Recommendations

ABSTRACT: The ever-growing demand for novel, cheaper, and more effective drugs has put nanomedicine and targeted drug delivery to the forefront of scientific innovation. Owing to its porous three-dimensional (3D)-nanostructure and properties, the biogenic calcite from wasted blue crab shells is employed in the present work as a new drug carrier for 5-fluorouracil (5-FU), a drug widely used in cancer therapy. The drug solution has been loaded in the porous nanoarchitecture of the powdered biogenic material and further pelleted in tablets with a 5-FU concentration of 1.748 mg/g. Their structural and morphological properties were characterized using Raman, X-ray diffraction, and scanning electron microscopy. Confocal micro-Raman spectra of tablet surface showed a typical signal of biogenic carbonate with preserved carotenoids and carotenoproteins found in the native waste shell, while the drug Raman signal was absent, indicating its adsorption in the intricate nanoporous biogenic carrier. The slow release of the drug from the newly formulated tablet was investigated by tracking the surface-enhanced Raman scattering (SERS) signal of the tablet solution in a series of time-dependent experiments. The SERS signal quantification is achieved using the well-known SERS spectral fingerprint of 5-fluorouracil aqueous solution adsorbed on Ag nanoparticles. The proof of concept is demonstrated by quantifying the slow release of the drug through the characteristic SERS band intensity of 5-FU in a time course of 26 h. This proof of concept boosted further investigations concerning the released drug identity in simulated solutions that mimic the pH of the upper- and lower gastrointestinal tract, as well as the multiple possibilities to control porosity and composition during powdering and treatment of biogenic material, to achieve the most convenient formulation for relevant biomedical drug delivery. Nonetheless, the present results showed great promise for innovative reusing waste biogenic 3D-nanomaterials of aquatic origin as advantageous drug carriers for slow release purposes, in line with the concept of blue bioeconomy.

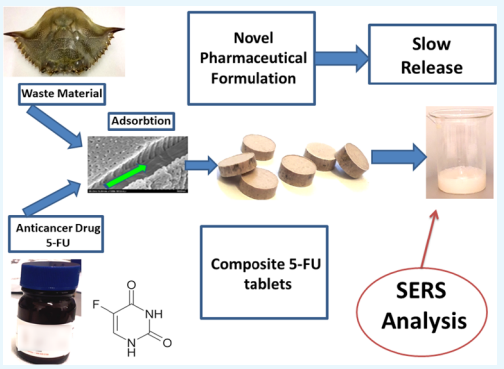

1. INTRODUCTION

Drug administration by an enteric route is a much desired delivery system as it provides the most accessible, convenient, and noninvasive method. However, in the case of certain pharmaceuticals, the enteric administration (via the gastrointestinal tract) poses serious difficulties. Drug decomposition by acids and enzymes in the gastrointestinal tract (GI), lack of specificity, and localized therapeutic action are only a few of the setbacks encountered using this delivery method.[1,2] To tackle these challenges, the adsorption of the drug on a carrier, followed by its slow release in the targeted region, seems to be the most viable alternative.[3−8] Research efforts are being focused on the development of new, cheap, and accessible materials capable of adsorbing and releasing sizeable amounts of material.[9−11] Enteric administration of pharmaceuticals can produce both systemic and local effects in the GI. The lower GI tract poses a series of challenges for developing efficient drug delivery systems, particularly in anticancer research.[12,13] Targeted colon drug delivery is highly desirable because of the benefits of a sufficient amount of treatment at the organ site.[12] Novel pharmaceutical formulations and nanostructured delivery systems are developed with the aim of increasing the efficiency and reducing the side effects of the drugs.[14−16] The targeted delivery to the lower GI tract implies that the drugs can successfully pass the stomach and upper intestinal tract and then be released at the colon site. The adsorption on a carrier followed by the slow local release of cytotoxic drugs such as 5-fluorouracil (5-FU), widely used to treat colon cancer, could significantly reduce the side effects while achieving high local therapeutic efficiency.[4,17−19]

Received: June 23, 2021
Accepted: September 9, 2021
Published: October 11, 2021

https://doi.org/10.1021/acsomega.1c03285
ACS Omega 2021, 6, 27781−27790

In the present work, an abundant yet largely unused biomaterial, the wasted shells of the Atlantic Blue Crab, *Callinectes Sapidus*, is proposed as a new drug carrier for 5-FU. Compared to other drug carriers derived from biogenic calcium carbonate,[20,21] the shell of the blue crab provides a series of advantages in terms of the physicochemical properties of the material, the preparation method, and availability. We recently showed that the shell of the blue crab is an intricate, highly ordered three-dimensional (3D)-nanoarchitecture of a magnesian calcite (Mg-$CaCO_3$) matrix with nanosized pores and channels and organic scaffolds comprising chitin−protein fibrils, rich in carotenoid pigments (astaxanthin), and carotenoproteins.[22] The porosity and hierarchical three-dimensional nanostructure of the crab shell architecture triggered the present work to prove its suitability for drug solution adsorption and subsequent active compounds release, which are the key factors that enable the use of such waste biomaterial in pharmaceutical formulation. The biocompatibility of the $CaCO_3$ is another major upside of the blue crab shell, which, coupled with the antioxidant properties conferred by the genuine carotenoid content of the biogenic material, not only does eliminate the risk of adverse side effects but could potentially offer further benefits in specific pharmaceutical formulations. Recent studies in our group have also shown that the biogenic material from crustacean shells maintains its porous nanostructure following mechanical or thermal processes, such as moderate heating or ball-milling powdering,[23] making it perfectly suitable for drug loading and biocompatible formulations.

Confocal Raman microspectroscopy (CRM) is employed here as a fast and nondestructive technique to characterize the composition of the biogenic powder before and after drug solution adsorption and pelleting in tablets the novel composite drug. Scanning electron microscopy (SEM), Brunauer−Emmett−Teller (BET) method, and X-ray diffraction (XRD) are used as complementary techniques for the analysis of the biogenic powder employed for drug loading. Furthermore, due to its high sensitivity and specificity, we chose surface-enhanced Raman scattering (SERS) as a novel and effective method to track the slow release of the 5-FU drug from the newly formulated tables suspended in water. SERS relies on the enhanced Raman scattering of molecules that are adsorbed on noble metal nanoparticles, which allows the detection of the substance at very low concentrations. Thus, the drug released in a solution of the suspended tablet is detected according to its characteristic SERS signature and quantified using the well-known SERS spectral fingerprint of 5-fluorouracil in water.[24,25] We used the drug of choice for the proof of concept and emphasized here the wider applicability of a wasted material such as the biogenic porous calcite from crustacean shells for solution loading, as we recently showed for the case of new, enriched biogenic calcite biofertilizers with loaded algae extracts.[26] We also showed[27] that the microbiological properties and heavy metal contents of the crustacean shells are compliant with such applications.

In the field of calcite particle applications, biogenic carbonates of aquatic origin showed an increased interest, mainly for microbial calcite. Coccolithophores were potentially speculated for wide applicability, such as drug fillers, painting materials, and others; however, their critical evaluation found such applicability not feasible[28] due to the small amount of coccoliths that could be experimentally harvested from natural seawater, relative to the costs and efforts to upscale such applications. On the contrary, crustacean calcite ultrastructure in 3D-nanoarchitecture poses obvious advantages in terms of availability and costs for sustainable, upscaled exploitation.

2. RESULTS AND DISCUSSION

Figure 1 depicts the steps performed in the preparation of the novel formulation of 5-FU, tablet characterization, and further

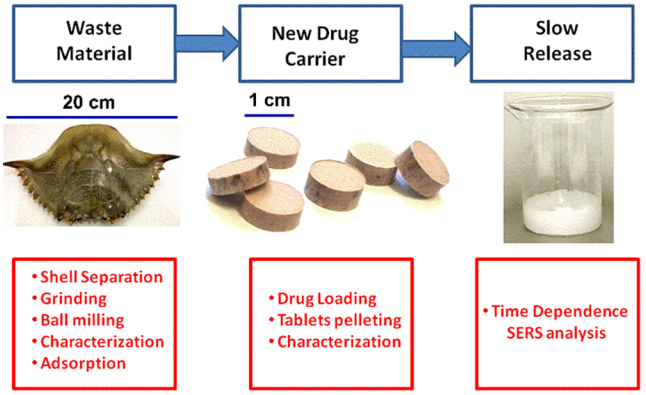

Figure 1. Graphical sketch of the experiments performed by loading 5-fluorouracil in nanoporous biogenic Mg-calcite powder from blue crab carapace and SERS detection of the released drug from tablets in solution.

investigation of their drug release in water solution using the ultrasensitive SERS technique for 5-FU detection.

Ball milling of the biogenic material for 3 or 5 min revealed minor differences in particle size distribution. N_2 adsorption−desorption isotherms and pore size distribution for blue crab carapace milled for 3 and 5 min, respectively, are shown in Figure 2. Both samples present BET surface areas below 10 m^2/g, with the carapace milled for 3 min exhibiting a higher value (7.17 m^2/g). The powdered carapace milled for 3 min exhibited a pore volume of 0.014 cm^3/g, while the one milled for 5 min exhibited 0.015 cm^3/g.

Investigated samples present isotherms of type IV characteristic to mesoporous materials (pore size nomenclature according to IUPAC classification), with the H3 type hysteresis loop, indicative for nonrigid aggregates of plate-like particles, or pore network consisting of macropores not completely filled with condensate[26] (N_2, in this particular case). Indeed, by analyzing the pore size distribution (Figure 2b,d), it may be observed that the samples show a nonuniform distribution of the pore widths, ranging from 3 to 60 nm. The broader size range is consistent with inherent variation in biological materials.

Nekvapil et al.[22] and references therein show that these pores in native shells are not spherical but are rather a network of elongated pillars, and also crab color specific, with thinnest porosity in the blue shell from crab claws. Here, considering carapace only, the pore diameter in milled carapace determined by the BET method is in the range of 3−60 nm, which is close to the size of pores in the native claw shells of the Atlantic blue crab (*C. sapidus*) and the Mediterranean green crab (*Cruoriopsis aestuarii*).[22]

The scanning electron microscopy (SEM) technique was employed for the examination of the powder particle morphology. The natural crab shells consist of a regular 3D network of calcium carbonate on an intricated chitin−protein scaffold. Such a network is crossed by channels and an array of

https://doi.org/10.1021/acsomega.1c03285
ACS Omega 2021, 6, 27781−27790

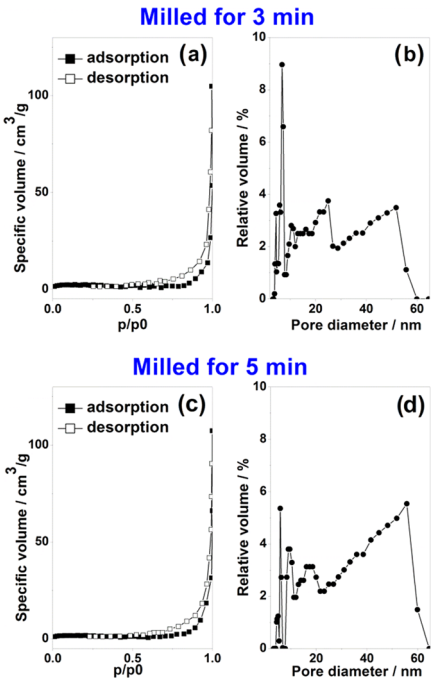

Figure 2. Powder porosity resulted from the blue crab (*C. sapidus*) carapace milled for 3 min (upper) and 5 min (lower), using the BET method with liquid nitrogen: (a) and (c) show adsorption and desorption isotherms, while (b) and (d) show the pore diameter distribution.

nanopillars separated by pores in the ultrastructure channel walls. The high-resolution SEM images revealed the nanopores and channel fragments in powder particles (Figure 3). Previous

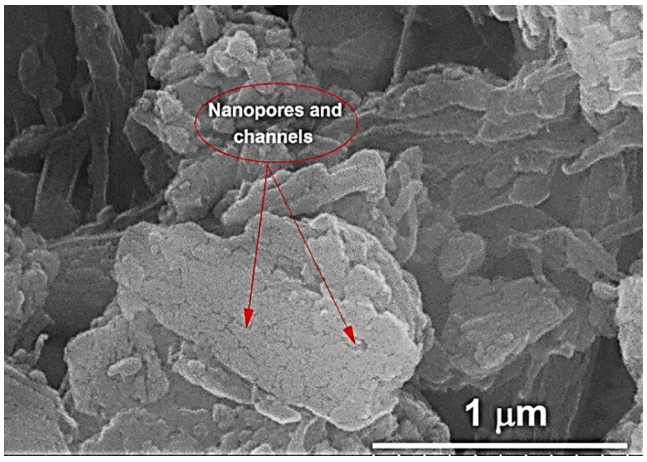

Figure 3. Scanning electron microscopy (SEM) image of the powder particles obtained by milling the blue crab carapace.

work in our group[22,23] demonstrated that the architecture at the nanoscale is preserved during mechanical grinding, enabling the easy loading of solutions into these nanopores. This unique feature of the blue crab shell powders is the foundation of the present work and provides various application domains.

A confocal Raman microspectrometer (CRM) was employed to analyze the powder composition after milling. As the Raman output of the blue crab shell is mainly composed of calcium carbonate along with carotenoid pigment signal,[22] two different excitation wavelengths were employed: one at 532 nm could resonantly excite the carotenoids, and a NIR line at 785 nm, which could provide nonresonantly an overall signature of all of the molecular compounds from sample. The presence of the carotenoids in biogenic powder was confirmed by the two main Raman bands at 1153 and 1516 cm^{-1} (Figure 4a)

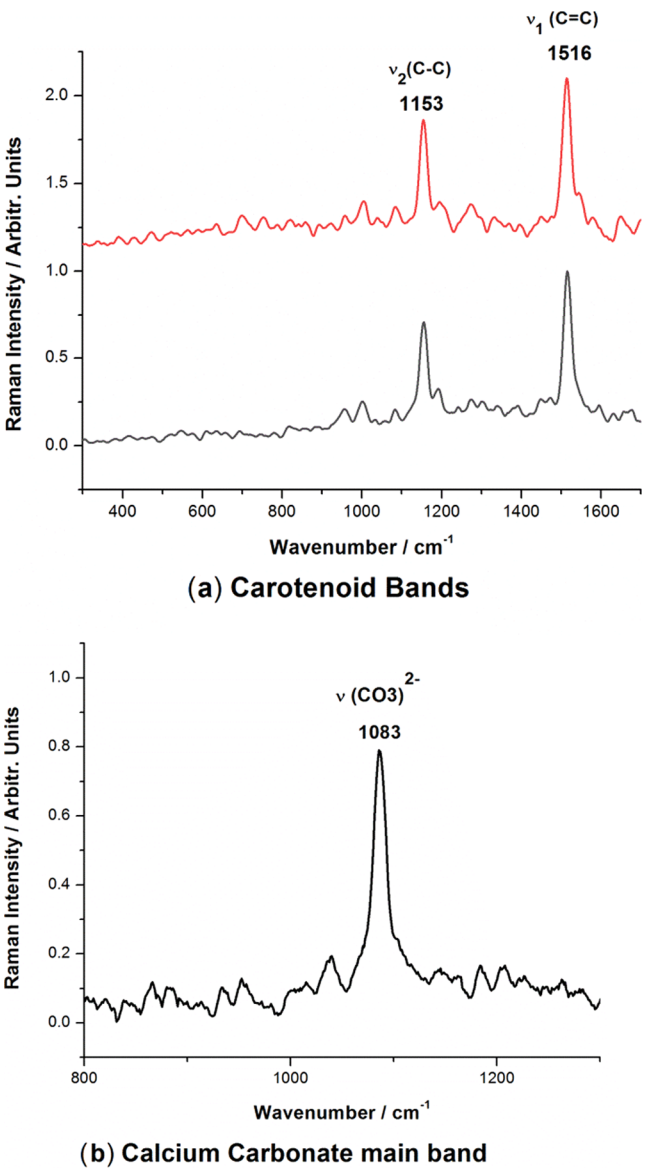

Figure 4. Raman spectra (background subtracted) of powder resulted from blue carapace showing the carotenoid preservation in both powdered samples in the case of Raman excitation with the 532 nm laser line (a) due to the resonance Raman effect selectively detecting carotenoids, while the carbonate signal only is detected under near-infrared laser excitation at 785 nm (b).

assigned to the characteristic C−C and C═C bonds of the skeletal chains. The NIR line at 785 excited the Raman signal of calcite with the main stretching mode of carbonate at 1085 cm^{-1} (Figure 4b).

A solution of 5-FU with 1 mg/mL concentration was then prepared to load the drug in the biogenic powder. Additionally, SERS measurements were performed on the 5-FU solution, and the results obtained were in good agreement with the previous SERS reports on this compound.[24,25] The main SERS

https://doi.org/10.1021/acsomega.1c03285
ACS Omega 2021, 6, 27781−27790

bands of 5-FU are present at 786, 1234, 1334, and 1667 cm^{-1} and are assigned to the pyrimidine ring breathing, the complex mode comprising ring + C−F wagging, ring + C−H wagging modes, and to the symmetrical stretching of the C═O bond, respectively. Their positions and relative intensities strongly depend on the pH and the concentration of the solution. Figure 5 comparatively shows the Raman spectrum of 5-FU

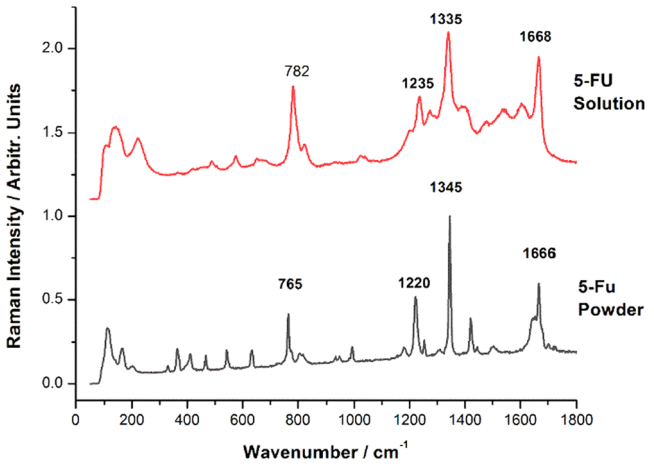

Figure 5. Micro-Raman spectrum of 5-FU powder (lower) compared to the SERS signal of the 5-FU solution (0.02 μg/mL) on AgNPs. Raman and SERS spectra were acquired using 1 s exposure time, 1 acquisition, 200 mW laser power, and a 20× magnification microscope objective. Excitation: 532 nm.

powder and the SERS spectrum of the 5-FU solution (1 mg/mL) used in this experiment, with the characteristic bands clearly visible. A typical process SERS spectrum recorded from the aqueous solution containing one suspended tablet is shown in Figure 6. The characteristic SERS bands of 5-FU were

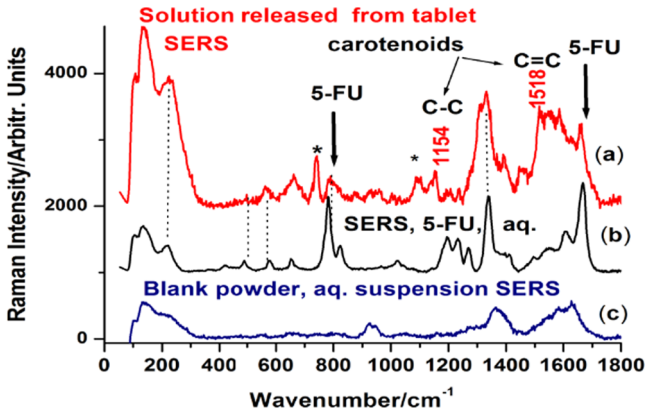

Figure 6. Typical SERS spectrum (background subtracted) recorded from the released solution from a tablet loaded with 5-FU (a) compared to the SERS of pure 5-FU aqueous solution (b) and the signal recorded from blank powder in water suspension (c). The * symbol denotes other bands from the biogenic composition.

observed along with a typical signature of carotenoid bands at 1518 and 1154 cm^{-1}, as indicated in Figure 6. Comparatively, a blank powder (not loaded with 5-FU) suspended in the aqueous solution and tested for SERS signal indicated a weak signal with dominant, broadened background peaking around 1600 and 1380 cm^{-1}.

3. CONCENTRATION-DEPENDENT SERS SPECTRA OF 5-FU

The main goal of this work is to study the release potential of 5-FU from the composite tablets in fluids compatible with biological organisms using the SERS signal of the drug. Therefore, prior to the slow release experiments, we investigated the variation of the SERS spectra of 5-FU as a function of its concentration in solution. Six different samples were prepared with concentrations ranging from 20 to 0.2 μg/mL. SERS spectra were collected for each of the solutions, and the data were analyzed to determine the quantitative analysis capability for the given range of concentrations via SERS. The raw Raman spectra were normalized, and for building a reliable quantitative SERS calibration curve, the SERS intensity measured as the area of the peak at 782 cm^{-1} was used. The normalized SERS spectra of the samples, along with the calibration curve, are shown in Figure 7. As the solution is diluted, the SERS intensity of the 5-FU signal continuously decreases, with the limit of detection lower than 0.2 μg/mL. The calibration curve resembles the dependence curve described by Farquharson et al.,[24] and it follows a

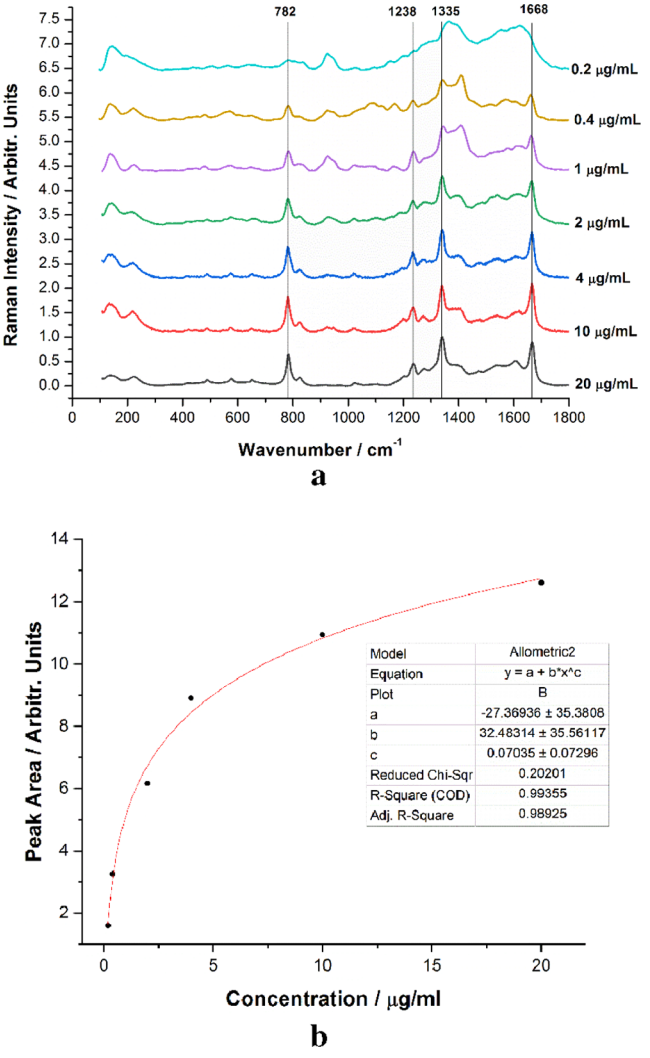

Figure 7. (a) Normalized SERS spectra of 5-FU at concentrations ranging from 0.2 to 20 μg/mL, with the main SERS bands tagged. (b) 782 cm^{-1} peak area plot against the concentration.

https://doi.org/10.1021/acsomega.1c03285
ACS Omega 2021, 6, 27781−27790

Langmuir−Blodgett type response as it is a function of available silver surface area. The peak area vs concentration plot was fitted following an allometric model, $y = a + b \cdot x^c$, with a COD (coefficient of determination) of 0.99. The resulting fitted curve was used as a reference in later experiments and calculations.

Images of the biogenic powder and 5-FU drug solutions before and after mixing are shown in Figure 8. It is noted that

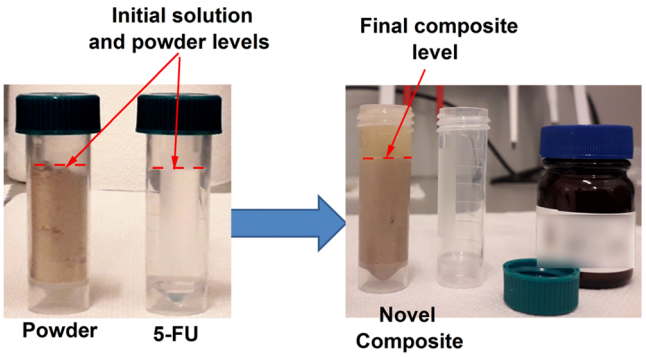

Figure 8. Images of the blue crab shell powder and 5-FU before (left) and after drug solution loading (right).

the capacity of adsorption of the porous powder from 5 mL volume of powder and 5 mL of 5-FU solution resulted in 6.5 mL of composite. Thus, the high capacity of biogenic calcite powder for solution loading is emphasized. The resulting mixture was a semifluid light brown composite, and its total volume of 6.5 mL was further used for tablet pelleting after drying.

Thicker or thinner tablets with masses ranging from 0.34 to 0.54 g were obtained and characterized using Raman microspectroscopy. As expected, Raman spectra collected from the surface of the tablets comprised the characteristic signal of the powdered shell (carotenoids and calcium carbonate), with no trace of the 5-FU signal, suggesting that the drug was incorporated into nanopores, thus, not signaling. To detect both the organic carotenoid pigments and the calcium carbonate, we used the same excitation wavelengths, 532 and 785 nm, the first relying on the resonance Raman effect to prove the carotenoid preservation in tablets, and the last, to characterize the matrix via NIR-Raman. The tablets along with their CRM spectra are shown in Figure 9.

Further XRD measurements were performed to consolidate the results obtained from the CRM analysis. The XRD analysis is presented in Figure 10. To examine the adsorption of the drug into the nanopores of the powder, the X-ray diffractogram of the 5-FU crystalline powder was recorded and compared to the pattern of the composite tablets' surface. Figure 10 clearly shows that the 5-FU spectral signature is absent from the tablet signal and the visible peaks were unambiguously assigned to Mg-calcite (marked with C on the graph), as described in detail in our previous study on the composition and morphology of the blue carb shell.[22] Unexpectedly, monohydrocalcite peaks (marked with MHC on the graph) were also observed and the origin of this mineral could be presumably explained by the co-existence of the amorphous calcium carbonate, which precipitates as MHC during tablet preparation where water is involved. A dedicated study on the occurrence of MHC in tablets will be necessary since MHC is not typical in the native crab shell.

The entire concept of the present study relies on two main assumptions: (1) the drug 5-FU is adsorbed in the nanopores

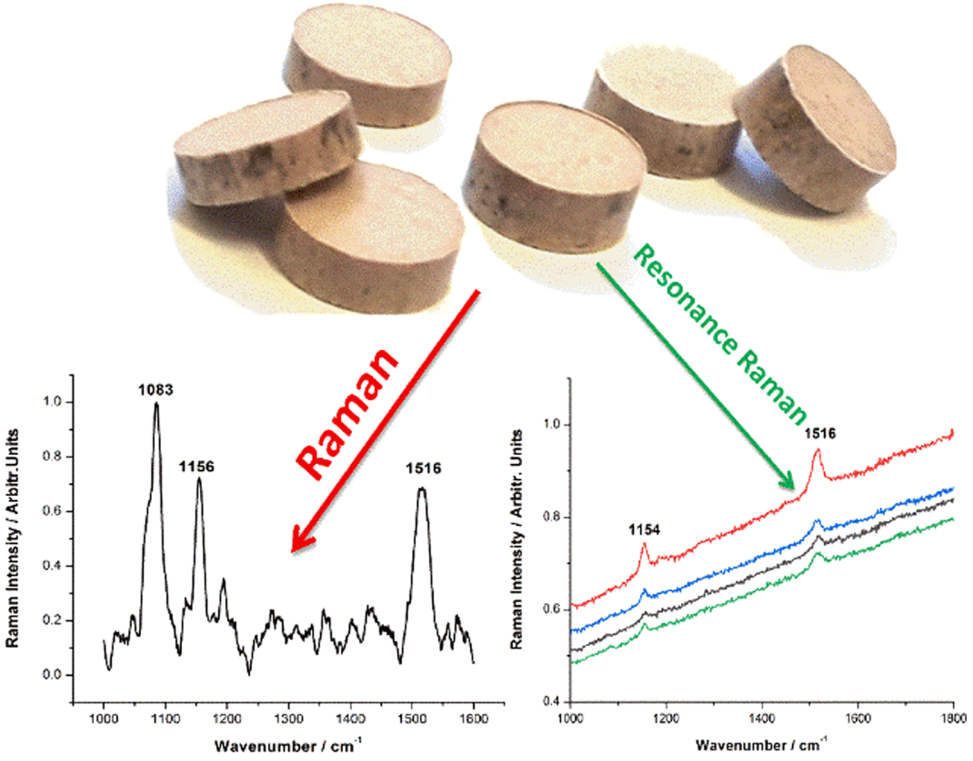

Figure 9. Image of the novel composite drug tablets and their typical raw Raman spectra collected from the tablet surface, indicating the presence of carotenoids (right) under 532 nm laser excitation and calcium carbonate (left), under 785 nm.

https://doi.org/10.1021/acsomega.1c03285
ACS Omega 2021, 6, 27781−27790

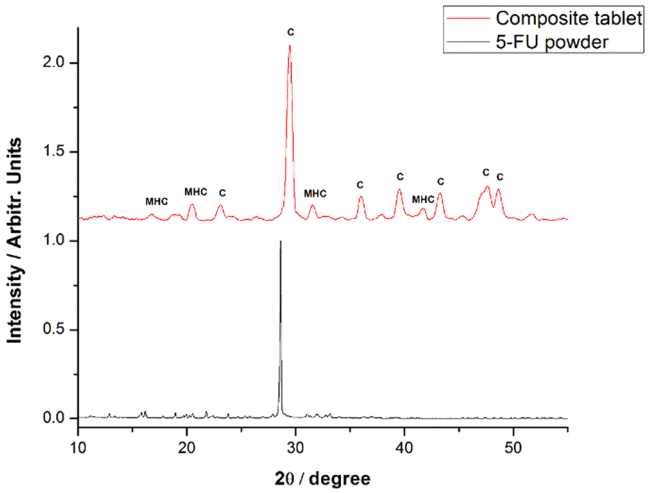

Figure 10. XRD pattern of the tablets (upper) revealing the crystalline calcite signal (marked with C on the graph) as well as the monohydrocalcite signal (marked with MHC) and (lower) of the pure 5-FU powder.

of the blue crab shell and (2) the drug is released from the nanopores when the composite tablets are suspended in fluids.

To characterize the tablets, confocal micro-Raman and XRD spectra were recorded from their surfaces. The results clearly showed that there is no trace of 5-FU at the surface and that the drug is adsorbed in the porous structure. To prove the second assumption, the slow release of 5-FU from the tablet was studied, exploiting the SERS capability to detect the trace amount of 5-FU released from the tablet suspended in water in a time-dependent experiment. The tablet stability in water was noted. Additional stirring was applied to stimulate its mechanical disintegration. For time-series SERS experiments, the composite tablets were suspended and stirred in ultrapure distilled water. A small amount of 10 μL of solution was collected from 10 to 10 min in the first hour, then further from hour to hour in the next 6 hours, with the final sample being collected after 26 h from the tablet suspension in water. SERS measurements were acquired in an effort to investigate the temporal dependence of the drug release. Figure 11a presents the averaged and normalized SERS spectra collected in the first hour at 10 min intervals, and Figure 11b presents the averaged and normalized SERS spectra collected from the tablet suspended solution in the following hours of the experiment, as indicated.

A blank SERS sample was prepared using the solution of ultrapure distilled water with suspended shell powder and further used for SERS analysis. Comparing the results shown in Figure 11a, it is clearly visible that the 5-FU signal was not detectable up to the end of the first hour of the experiment suggesting that the amount of 5-FU released is below the current SERS detection limit. The presence of the most intense bands of the solution background, at 1367 and 1620 cm^{-1}, in close proximity of the main 5-FU bands (1238, 1335, and 1668 cm^{-1}) makes it difficult to detect the drug as its SERS response signal is hampered by the background induced by organic components of powder. Starting from the second hour, the SERS response signal of 5-FU becomes more pronounced in samples collected from the solution. The characteristic bands at 782, 1228, 1335, and 1668 cm^{-1} are clearly visible in every spectrum, with increasing intensities as the experiment timely progressed. Using the previously presented calibration curve

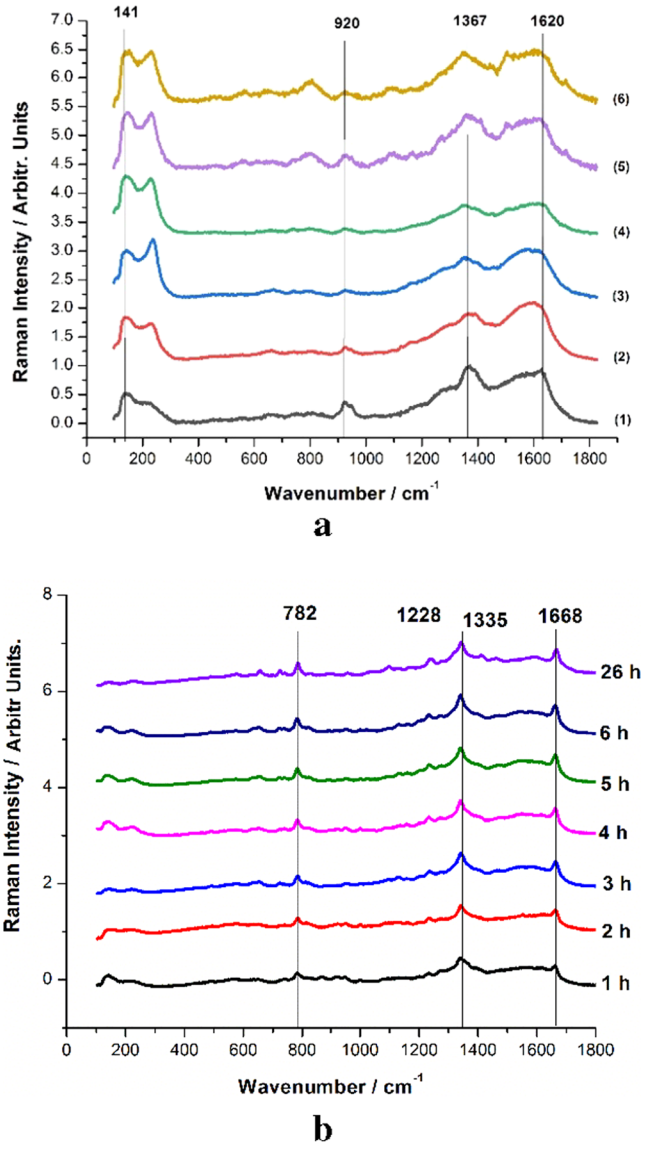

Figure 11. Averaged and normalized SERS spectra of the samples collected from the solution containing the tablet in the first hour (a) and in the following 5.5 h (b). The SERS spectra from the blank powder suspended in water are given in the bottom line of (a) and denoted as (1). The numbers indicate the SERS of solutions taken after 10 (2), 20 (3), 30 (4), 40 (5), and 50 min (6).

for the pure 5-FU solution (Figure 7b) as a reference, the variation of the 782 cm^{-1} peak area over time allowed the quantification of the 5-FU released from the tablet as a function of concentration. The results are shown in Figure 12.

The 782 cm^{-1} peak area was calculated for every spectrum collected from each sample, the results were averaged, and the relative error was calculated for each sample. By correlating the results with the previously discussed calibration curves for the 5-FU solution (Figure 7), the amount released was quantified and plotted against the time, with the 5-FU released given as a percentage of the total amount of drug contained in the tablet. As mentioned, no 5-FU release could be detected in the first hour of the experiment; however, after the first hour, the released amount had built up to an average of approximately 40%, suggesting a slow release in the first hour but insufficient to surpass the detection limit. The release process continued over the next few hours, reaching a total amount of

https://doi.org/10.1021/acsomega.1c03285
ACS Omega 2021, 6, 27781−27790

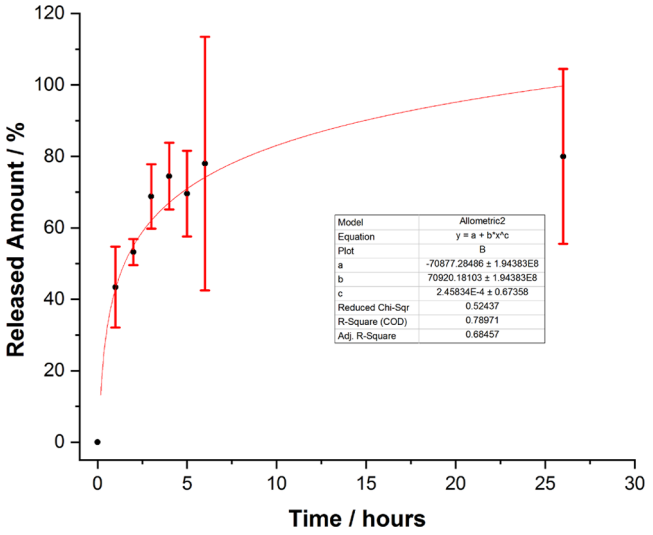

Figure 12. Released amount of FU from the tablet as a function of time.

approximately 80% released in 6 hours. However, the results obtained for this time period are less precise and are subject to larger relative errors. After the 6th hour, the release process had seemingly ceased, as the concentration of 5-FU in the solution was roughly the same after one day. The latter errors could be attributed to additional readsorption processes on the biogenic particles from the solution. Presumably, the amount released had reached its peak and the process had seized after the 6th hour because the tablet had almost entirely released the material it was loaded with. The released amount vs time plot seemingly follows the same allometric growth pattern as in Figure 7b, although the COD is much lower, 0.78, due to the large relative errors. It is expected that the function, released amount of drug over time, would not perfectly fit with any mathematical expression due to the large number of factors influencing it at the interface of water-biogenic nanoparticles and drug, on the one hand, and due to the SERS slightly modified interaction, on the other hand, as the test solution on AgNPs slightly changes its properties in time. Nevertheless, the proof of concept regarding the adsorption of drug solution in biogenic powder from blue crab and its subsequent release has been proved for the first time here. The ability and convenience of the SERS technique to track such releasing processes from loaded biogenic calcite nanoformulations should be highlighted.

4. CONCLUSIONS AND OUTLOOK

In the present work, we have proven so far that the biogenic calcium carbonate from the shell of the Atlantic blue crab has a great potential to be used as a drug carrier due to its 3D-porous nanoarchitecture and content of major, biocompatible Mg-calcite and natural antioxidants embedded in its highly ordered nanostructure. Moreover, we have also demonstrated that SERS can be used as a feasible method to study the release process of substances, such as the anticancer drug 5-FU, loaded in biogenic calcite particles. The use of the blue crab shell as a drug carrier presents numerous advantages compared to other classical formulations. The loading process is relatively simple, and the shell needs minimal physical preparation (powdering) prior to its loading with a drug solution, making the preparation of a large number of composite tablets in a short time period possible. Moreover, its biocompatibility and carotenoid content enrich beneficial side effects and could bring further innovative solutions for the targeted delivery of 5-FU to the lower digestive tract in the treatment of colon cancer. Thus, the proof of concept is being demonstrated by quantifying the characteristic SERS band intensity of 5-FU in a time course of 26 h, further experiments regarding the influence of the preparation parameters, such as particle dimension optimal for certain drug solution concentrations, amount of drug loaded, tablet size optimization, and the influence of external parameters, such as pH and temperature, on the adsorption and release process of the drug, are still underway, with particular emphasis on the drug release in the biological fluid environment.

The blue crab shell possesses a series of advantages compared to other carriers, regarding both the physical properties of the material, as well as the preparation method and economic aspects of its implementation on a large scale. The shell is mainly composed of a biogenic calcium carbonate matrix; thus, it is biocompatible, while the chitin is generally considered as safe. What makes it more attractive for reusing as drug carriers is the natural antioxidant character due to the natural distribution of carotenoids (free and noncovalently bound astaxanthin in carotenoproteins) in shells. We have just demonstrated in previous papers that two pigments are preserved during the mechanical treatment or careful thermal process.[22,23] Thus, carotenoids and carotenoproteins provided additional benefic effects of such materials used as drug carriers. Besides, the preparation procedure is relatively simple, can be performed with relatively accessible equipment, and, importantly, is easily scalable for industrial use. Finally, unlike other carriers, the blue crab shell is a cheap and accessible waste material. Its use as a drug carrier falls in line with the concepts of the circular economy and blue bioeconomy.

This work reported the proof of concept in reusing powders from biogenic waste material to develop novel and reliable nanocomposites for drug carriers, and the new formulations could be tracked regarding drug adsorption and subsequent release using a novel approach based on the sensitive SERS technique. The anticancer drug 5-fluorouracil was used just as an example of the drug for the proof of concept. Thus, being aware of the need for further research regarding particular drug for specific targeting particular segments of the digestive tract, further developments are certainly necessary regarding the preparation of the composite drug (5-Fu loaded in the carrier), in terms of biogenic powder physical−chemical properties, pelleting force, size of pellets, and the loaded 5-FU quantity as a function of such variables. These studies are in due course, considering both the deproteinized and nondeproteinized biogenic material. The present paper just proves that the concept of the work is viable, and we are currently studying the behavior of the composite in acid pH to simulate the application environment.

The present results certify the wide applicability of such biogenic materials for solution loading and slow release, thus boosting novel, innovative applications based on advanced knowledge on their properties, according to the bioeconomy priorities.

5. MATERIALS AND METHODS

5.1. Materials. 5-Fluorouracil, in the form of a 99% purity powder (Merck), was purchased from Nordic Chemicals (Cluj-Napoca, Romania) and was used without further

https://doi.org/10.1021/acsomega.1c03285
ACS Omega 2021, 6, 27781−27790

purification. Specimens of the Atlantic blue crab, *C. sapidus*, were caught in the Parila Lagoon, within the Neretva river delta (Croatia; south-east Adriatic Sea). The medium-sized crabs caught (10−15 cm carapace width) were frozen at −20 °C until further preparation.

5.2. Methods. *5.2.1. Shell Powder Preparation.* Crabs were thawed, dissected, and the soft tissue was removed using the dissection equipment (scissors, tweezers, and scalpels). Thereafter, the shells were carefully rinsed in warm water (<30 °C) to obtain clean biogenic carbonate structures from the blue-colored crab claws and the carapace. One gram of shell samples was roughly ground in for further milling purposes, using only the blue claw and the carapace shells (4 milling trials in total) from the total shell waste.

5.2.2. Obtaining Biogenic Powder and Particle Characterization. Following intensive cleaning and washing, the crab shell was removed and mechanically ground to centimeter size fragments for subsequent ball milling. The ball-milling technique was employed to turn the shell into a fine powder with the particle size in the micro-nano range, using a Fritsch Pulverisette 4 planetary ball mill. The 80 mL hardened steel vials were used, with 13 balls of 10 mm steel diameter per vial. Two different milling times, 3 min and 5 min, were used to compare the effect of the milling time on the size of the powder particles. Nitrogen physisorption analysis was performed by means of the Sorptomatic 1990 equipment (Thermo Electron) to evaluate the specific surface area, pore volume, and pore size distribution of the powders from the blue crab carapace. Before N_2 adsorption at −196 °C, the samples were pretreated by degassing under vacuum, at 150 °C, for 4 h (temperature rate of 2 °C/min from room temperature to final temperature). The specific surface area of the samples was estimated from the adsorption isotherm in the relative pressure interval of 0.01−0.25 p/p0, according to the standard BET procedure.[29] The specific pore volume was evaluated using the Dollimore−Heal method, while the mean pore widths were estimated using the desorption branch in the 0.01−0.95 p/p0 range.

5.2.3. Tablet Preparation and SERS Analysis. A stock solution of 5-FU, which was used throughout the experiments, was prepared by dissolving 50 mg of 99% purity 5-FU powder in ultrapure distilled water (18.2 M ohm), resulting in a solution of 1 mg/mL concentration. Five milliliters of 5-FU solution has been added to an equivalent volume of powdered blue crab carapace, milled for 5 min. The powder volume of 5 mL weighing 3.659 g easily loaded the 5-FU solution in the nanopores of the powder, resulting in a total volume of 6.5 mL of a semifluid light brown composite. The composite was left to dry at room temperature (20 °C), and the resulting solid mass was pressed into six tablets weighing 2.86 g in total, using 3 ton force mechanical press. The tablet diameter was 10 mm. The total dried mass of the six tablets was 2.86 g, bearing 5 mg of 5-FU, thus resulting in a tablet drug concentration of 1.748 mg/g.

5.2.4. SERS Quantification of 5-FU Released from Tablets. In a time-series experiment, each tablet was individually suspended in 25 mL of distilled water under continuous stirring at room temperature (20 °C). As such, the obtained solution from each tablet was tested for the occurrence of the 5-FU SERS signal by probing a small amount of 10 μl of solution taken at different time intervals, as further described. For SERS sample preparation, the test solution under stirring was tested periodically by adding it to 500 μL of colloidal silver nanoparticles (AgNPs) prepared according to the classical, Lee-Meisel procedure (citrate-reduced colloidal $AgNO_3$).[30] The optical properties of the AgNPs were consistent with the previous characterization.[30,31] SERS spectra were recorded three times for each aliquot. SERS samples, in all experiments on all tablets, were identically prepared (10 μL of test solution with 500 μL of AgNPs). Preliminary SERS tests of the AgNPs were conducted using well-known SERS molecular species, such as methylene blue or 4-aminothiophenol, to check the SERS efficiency of the AgNPs, and their output was confirmed by recording the expected SERS feature as widely described in the literature. The absorbance maximum of the freshly prepared AgNPs was at 418 nm. Thus, the concentration of 5-FU in the tablet solution could be tracked, provided that the SERS signal quantification could theoretically be achieved for concentrations lower than 20 μg/mL.

5.2.5. Instruments and Data Processing. Confocal Raman and SERS spectra were acquired using a Renishaw InVia Confocal Raman System and a Cobolt DPSS laser emitting at 532 nm, as well as a high power NIR diode laser emitting at 785 nm. During Raman microscopy, the 5× (NA 0.12 WD 13.2 mm), 20× (NA 0.35, WD 2 mm), and 100× (NA 0.9, WD 3.4 mm) collecting objectives were used with theoretical spatial resolutions of 2.7, 0.927, and 0.36 μm, respectively. For SERS spectra acquisitions, the 20× (NA 0.35, WD 2 mm) objective and the 532 nm laser line were used, with the acquisition parameters of 20 s exposure time, 1 acquisition, 200 mW laser power. An edge filter has been employed to record spectra in the 90−1840 cm^{-1} spectral range with 0.5 cm^{-1} resolution. The signal has been detected using a Rencam CCD, and data acquisition and processing have been achieved with WIRE 3.4 and OriginPro 8.5 software.

Scanning electron microscopy (SEM) imaging of the shell powder was conducted on a Hitachi SU8230 cold-field emission electron microscope. The samples were deposited on a carbon SEM stub holder sputter-coated with a 7−10 nm thick Au film prior to imaging.

The composition of the pellets was probed by X-ray diffraction (XRD), using a Bruker D8 Advance diffractometer in Bragg−Brentano geometry with a Cu tube with $\lambda K\alpha$ = 0.15418 nm, Ni filter, and a LynxEye detector. Corundum (NIST SRM1976a) was used as an internal standard. The data were collected on a 10−64° 2θ interval at a 0.02° 2θ step, measuring each step for 1 s. The identification of mineral phases was performed with Diffrac.Eva 2.1 software (Bruker AXS) using the PDF2 (2012) database.

AUTHOR INFORMATION

Corresponding Author

Simona Cinta Pinzaru − *Biomolecular Physics Department, Babes Bolyai University, RO-400084 Cluj-Napoca, Romania; Institute for Research, Development and Innovation in Applied Natural Science, 400327 Cluj-Napoca, Romania;* orcid.org/0000-0001-8016-4408; Email: simona.pinzaru@ubbcluj.ro

Authors

Geza Lazar − *Biomolecular Physics Department, Babes Bolyai University, RO-400084 Cluj-Napoca, Romania; Institute for Research, Development and Innovation in Applied Natural Science, 400327 Cluj-Napoca, Romania*

Fran Nekvapil − *Biomolecular Physics Department, Babes Bolyai University, RO-400084 Cluj-Napoca, Romania;*

https://doi.org/10.1021/acsomega.1c03285
ACS Omega 2021, 6, 27781−27790

Institute for Research, Development and Innovation in Applied Natural Science, 400327 Cluj-Napoca, Romania; orcid.org/0000-0001-8652-8292

Razvan Hirian − *Babes Bolyai University, Faculty of Physics, RO-400084 Cluj-Napoca, Romania*

Branko Glamuzina − *Department of Aquaculture, University of Dubrovnik, 20 000 Dubrovnik, Croatia*

Tudor Tamas − *Department of Geology, Babeş-Bolyai University, RO-400084 Cluj-Napoca, Romania*

Lucian Barbu-Tudoran − *Electron Microscopy Centre, Babes;-Bolyai University, 400006 Cluj-Napoca, Romania; Advanced Research and Technology Center for Alternative Energy, National Institute for Research and Development of Isotopic and Molecular Technologies, 400293 Cluj-Napoca, Romania*

Complete contact information is available at: https://pubs.acs.org/10.1021/acsomega.1c03285

Author Contributions

This manuscript was written through contributions of all authors. All authors have given approval to the final version of the manuscript.

Funding

This work was supported by a grant from the Ministry of Research, Innovation and Digitization, CNCS/CCCDI—UEFISCDI, project number PN-III-P2−2.1-PED-2019−4777, Nr. 377, within PNCDI III.

Notes

The authors declare no competing financial interest.

■ ACKNOWLEDGMENTS

G.L. additionally acknowledges the special Scholarship Grant of Babes-Bolyai University for scientific activity 2019−2020. F.N. acknowledges the Grant for Young Researchers 2019/2020, provided by the Babes;-Bolyai University, contract no. 31992/02.06.2020. Special thanks to Stanko from Parilla Lagoon, Croatia, for providing captured crabs whenever it was needed. The authors kindly acknowledge the BET measurements conducted by Dr. Maria Miheţ (the National Institute for Research and Development of Isotopic and Molecular Technologies, Cluj-Napoca).

■ REFERENCES

(1) Focaccetti, C.; Bruno, A.; Magnani, E.; Bartolini, D.; Principi, E.; Dallaglio, K.; Bucci, E. O.; Finzi, G.; Sessa, F.; Noonan, D. M.; Albini, A. Effects of 5- fluorouracil on morphology, cell cycle, proliferation, apoptosis, autophagy and ROS production in endothelial cells and cardiomyocytes. *PLoS One* **2015**, *10*, No. e0115686.

(2) Mohamed, H. S.; Dahy, A. A.; Mahfouz, R. M. Isoconversional approach for non-isothermal decomposition of un-irradiated and photon-irradiated 5-fluorouracil. *J. Pharm. Biomed. Anal.* **2017**, *145*, 509−516.

(3) Luo, H.; Ji, D.; Li, C.; Zhu, Y.; Xiong, G.; Wan, Y. Layered nanohydroxyapatite as a novel nanocarrier for controlled delivery of 5-fluorouracil. *Int. J. Pharm.* **2016**, *513*, 17−25.

(4) Hazrati, M. K.; Javanshir, Z.; Bagheri, Z. B 24 N 24 fullerene as a carrier for 5-fluorouracil anti-cancer drug delivery: DFT studies. *J. Mol. Graphics Modell.* **2017**, *77*, 17−24.

(5) Zatta, K. C.; Frank, L. A.; Reolon, L. A.; Amaral-Machado, L.; Egito, E. S. T.; Gremião, M. P. D.; Pohlmann, A. R.; Guterres, S. S. An Inhalable Powder Formulation Based on Micro- and Nanoparticles Containing 5-Fluorouracil for the Treatment of Metastatic Melanoma. *Nanomaterials* **2018**, *8*, 75.

(6) Sonker, N.; Bajpai, J.; Bajpai, A. K. Magnetically responsive release of 5-FU from superparamagnetic egg albumin coated iron oxide core-shell nanoparticles. *J. Drug Delivery Sci. Technol.* **2018**, *47*, 240−253.

(7) Zhang, L.; Xing, Y.; Gao, Q.; Sun, X.; Zhang, D.; Cao, G. Combination of NRP1-mediated iRGD with 5-fluorouracil suppresses proliferation, migration and invasion of gastric cancer cells. *Biomed. Pharmacother.* **2017**, *93*, 1136−1143.

(8) Kayumova, R. R.; Sultanbaev, A. V.; Ostakhov, S. S.; Khursan, S. L.; Abdullin, M. F.; Gantsev, S. K.; Sakaeva, D. D. The ≪ in vivo≫ study of blood 5-fluorouracil content by quenching of intrinsic protein fluorescence. *J. Luminescence* **2017**, *192*, 424−427.

(9) Fuster, M. G.; Carissimi, G.; Montalbán, M. G.; Víllora, G. Improving Anticancer Therapy with Naringenin-Loaded Silk Fibroin Nanoparticles. *Nanomaterials* **2020**, *10*, 718.

(10) Fratoddi, I.; Venditti, I.; Battocchio, C.; Carlini, L.; Amatori, S.; Porchia, M.; Tisato, F.; Bondino, F.; Magnano, E.; Pellei, M.; Santini, C. Highly Hydrophilic Gold Nanoparticles as Carrier for Anticancer Copper(I) Complexes: Loading and Release Studies for Biomedical Applications. *Nanomaterials* **2019**, *9*, 772.

(11) Deng, S.; Cui, C.-X.; Duan, L.; Hu, L.; Yang, X.; Wang, J.-C.; Qu, L.-B.; Zhang, Y. Anticancer Drug Release System Based on Hollow Silica Nanocarriers Triggered by Tumor Cellular Microenvironments. *ACS Omega* **2021**, *6*, 553−558.

(12) Auriemma, G.; Mencherini, T.; Russo, P.; Stigliani, M.; Aquino, R. P.; Del Gaudio, P. Prilling for the development of multi-particulate colon drug delivery systems: Pectin vs. pectin−alginate beads. *Carbohydr. Polym.* **2013**, *92*, 367−373.

(13) Galindo-Rodriguez, S. A.; Allemann, E.; Fessi, H.; Doelker, E. Polymeric nanoparticles for oral delivery of drugs and vaccines: a critical evaluation of in vivo studies. *Crit. Rev. Ther. Drug Carrier Syst.* **2005**, *22*, 419−464.

(14) Gaucher, G.; Satturwar, P.; Jones, M. C.; Furtos, A.; Leroux, J. C. Polymeric micelles for oral drug delivery. *Eur. J. Pharm. Biopharm.* **2010**, *76*, 147−158.

(15) Ferrari, P. C.; Souza, F. M.; Giorgetti, L.; Oliveira, G. F.; Ferraz, H. G.; Chaud, M. V.; Evangelista, R. C. Development and in vitro evaluation of coated pellets containing chitosan to potential colonic drug delivery. *Carbohydr. Polym.* **2013**, *91*, 244−252.

(16) Maroni, A.; Del Curto, M. D.; Zema, L.; Foppoli, A.; Gazzaniga, A. Film coatings for oral colon delivery. *Int. J. of Pharm.* **2013**, *457*, 372−394.

(17) Vilaça, N.; Amorim, R.; Machado, A. F.; Parpot, P.; Pereira, M. F.; Sardo, M.; Rocha, J.; Fonseca, A. M.; Neves, I. C.; Baltazar, F. Potentiation of 5-fluorouracil encapsulated in zeolites as drug delivery systems for in vitro models of colorectal carcinoma. *Colloids Surf., B* **2013**, *112*, 237−244.

(18) Abukhadra, M. R.; Refay, N. M.; El-Sherbeeny, A. M.; El-Meligy, M. A. Insight into the Loading and Release Properties of MCM-48/Biopolymer Composites as Carriers for 5-Fluorouracil: Equilibrium Modeling and Pharmacokinetic Studies. *ACS Omega* **2020**, *5*, 11745−11755.

(19) Iafisco, M.; Delgado-Lopez, J. M.; Varoni, E. M.; Tampieri, A.; Rimondini, L.; Gomez-Morales, J.; Prat, M. Cell Surface Receptor Targeted Biomimetic Apatite Nanocrystals for Cancer Therapy. *Small* **2013**, *9*, 3834−3844.

(20) Yao, Y.-Y.; Gedda, G.; Girma, W. M.; Yen, C.-L.; Ling, Y.-C.; Chang, J.-Y. Magnetofluorescent Carbon Dots Derived from Crab Shell for Targeted Dual-Modality Bioimaging and Drug Delivery. *ACS Appl. Mater. Interfaces* **2017**, *9*, 13887−13899.

(21) Render, D.; Samuel, T.; King, H.; Vig, M.; Jeelani, S.; Babu, R. J.; Rangari, V. Biomaterial-Derived Calcium Carbonate Nanoparticles for Enteric Drug Delivery. *J. Nanomaterials* **2016**, *2016*, No. 3170248.

(22) Nekvapil, F.; Pinzaru, S. C.; Barbu−Tudoran, L.; Suciu, M.; Glamuzina, B.; Tamas, T.; Chis, V. Color-specific porosity in double pigmented natural 3d-nanoarchitectures of blue crab shell. *Sci. Rep.* **2020**, *10*, No. 3019.

(23) Nekvapil, F.; Aluas, M.; Barbu-Tudoran, L.; Suciu, M.; Bortnic, R.-A.; Glamuzina, B.; Cîntă Pinzaru, S. From Blue Bioeconomy toward Circular Economy through High Sensitivity Analytical

Research on Waste Blue Crab Shells. *ACS Sustainable Chem. Eng.* **2019**, *7*, 16820−16827.
(24) Farquharson, S.; Gift, A.; Shende, C.; Inscore, F.; Ordway, B.; Farquharson, C.; Murren, J. Surface-enhanced Raman Spectral Measurements of 5-Fluorouracil in Saliva. *Molecules* **2008**, *13*, 2608−2627.
(25) Pavel, I.; Cota, S.; Cînta-Pînzaru, S.; Kiefer, W. Raman, Surface Enhanced Raman Spectroscopy, and DFT Calculations: A Powerful Approach for the Identification and Characterization of 5-Fluorouracil Anticarcinogenic Drug Species. *J. Phys. Chem. A* **2005**, *109*, 9945−9952.
(26) Nekvapil, F.; Ganea, I.-V.; Ciorîţă, A.; Hirian, R.; Tomšić, S.; Martonos, I. M.; Cintă Pinzaru, S. A New Biofertilizer Formulation with Enriched Nutrients Content from Wasted Algal Biomass Extracts Incorporated in Biogenic Powders. *Sustainability* **2021**, *13*, 8777.
(27) Nekvapil, F.; Ganea, I.-V.; Ciorîţă, A.; Hirian, R.; Ogresta, L.; Glamuzina, B.; Roba, C.; Cintă Pinzaru, S. Wasted Biomaterials from Crustaceans as a Compliant Natural Product Regarding Microbiological, Antibacterial Properties and Heavy Metal Content for Reuse in Blue Bioeconomy: A Preliminary Study. *Materials* **2021**, *14*, 4558.
(28) Jakob, I.; Chairopoulou, M. A.; Vučak, M.; Posten, C.; Teipel, U. Biogenic calcite particles from microalgae—Coccoliths as a potential raw material. *Eng. Life Sci.* **2017**, *17*, 605−612.
(29) Thommes, M.; Kaneko, K.; Neimark, A. V.; Olivier, J. P.; Rodriguez-Reinoso, F.; Rouquerol, J.; Sing, K. S. W. Physisorption of gases, with special reference to the evaluation of surface area and pore size distribution (IUPAC Technical Report). *Pure Appl. Chem.* **2015**, *87*, 1051−1069.
(30) Lee, P. C.; Meisel, D. Adsorption and surface-enhanced Raman of dyes on silver and gold sols. *J. Phys. Chem. A* **1982**, *86*, 3391−3395.
(31) Pinzaru, S. C.; Müller, Cs.; Tomšić, S.; Venter, M. M.; Brezestean, I.; Ljubimir, S.; Glamuzina, B. Live diatoms facing Ag nanoparticles: surface enhanced Raman scattering of bulk cylindrotheca closterium pennate diatoms and of the single cells. *RSC Adv.* **2016**, *6*, 42899−42910.

https://doi.org/10.1021/acsomega.1c03285
ACS Omega 2021, 6, 27781−27790